One-loop electroweak radiative corrections to polarized $e^+e^- \to ZH$

S. Bondarenko*
Bogoliubov Laboratory of Theoretical Physics, JINR, Dubna, 141980 Russia

Ya. Dydyshka,† L. Kalinovskaya, L. Rumyantsev,‡ R. Sadykov, and V. Yermolchyk†
Dzhelepov Laboratory of Nuclear Problems, JINR, Dubna, 141980 Russia

(Received 22 May 2019; published 4 October 2019)

In this paper we give high-precision theoretical predictions for cross sections of the process $e^+e^- \to ZH$ for future electron-positron colliders. The calculations are performed using the SANC system. They include complete one-loop electroweak radiative corrections, as well as the longitudinal polarization of initial beams. Numerical results are given for the center-of-mass energy range $\sqrt{s} = 250$–1000 GeV with various polarization degrees.

DOI: 10.1103/PhysRevD.100.073002

I. INTRODUCTION

The clean signatures of the reactions at e^+e^- colliders combined with the polarization effect of initial particles can increase the precision of theoretical predictions for various observables of Standard Model processes [1].

Future linear collider projects such as ILC [2] and CLIC [3] are designed to produce polarized beams—up to 80% for electrons and 60% for positrons. The prospects for beam polarization have also been considered for future circular colliders, such as CEPC [4] and FCC-ee [5]. The center-of-mass (c.m.) energy range of the above colliders will be $\sqrt{s} = 250$–1000 GeV, while 250 GeV is the optimal value for Higgs production through the Higgsstrahlung process $e^+e^- \to ZH$, which is the most important for obtaining precise measurements of the Higgs' mass, spin, CP nature, the coupling of the Higgs to ZZ, and various branching ratios. Thus, it is important to take beam polarization into account in theoretical calculations.

There are three main Higgs production processes at e^+e^- colliders: Higgsstrahlung ($e^+e^- \to ZH$), W fusion [$e^+e^- \to \bar{\nu}_e\nu_e(W^+W^-) \to \bar{\nu}_e\nu_e H$], and Z fusion ($e^+e^- \to e^+e^-(ZZ) \to e^+e^-H$) [6–12].

In this paper we present the results for the complete one-loop electroweak (EW) radiative corrections (RCs) to Higgsstrahlung for arbitrary longitudinal polarization of the positron and electron beams. Numerical results are obtained for various polarization degrees.

The radiative corrections to Higgsstrahlung with unpolarized initial particles were extensively considered in the literature [13–15]. Recently, the mixed QCD-EW corrections for Higgs boson production were estimated in Refs. [16,17]. The QED corrections due to the initial-state radiation to associated Higgs boson production in electron-positron annihilation by applying the QED Structure Function approach were recently evaluated in Ref. [18]. The polarized virtual and soft photon EW RCs to the Higgsstrahlung process were calculated in Refs. [19,20].

We present numerical estimations for the corrections of the total cross section and differential distribution in the Z-boson scattering angle $\cos\vartheta_Z$ as well as for the left-right asymmetry A_{LR} as a function of $\cos\vartheta_Z$. The relevant contributions to the cross section of the reaction are calculated analytically and numerically.

For the numerical evaluation of the process we use the MCSANC integrator [21,22] which has been extended for the longitudinally polarized e^+ and e^- beams (MCSANCEE integrator). It was previously used for the Bhabha process [23]. The unpolarized virtual and soft bremsstrahlung contributions are compared with the results of Refs. [19,20] and the GRACE-LOOP program [24]. The cross sections for the polarized Born and hard bremsstrahlung are verified by means of the corresponding results of the WHIZARD [25] and CALCHEP [26] programs.

The paper is organized as follows. In Sec. II we describe the cross section calculation technique at the one-loop EW level. Expressions for the covariant (CA) and helicity amplitudes (HA) are presented. The approach to take the polarization effects into account is discussed. In Sec. III we give numerical results for the total and differential cross sections as well as for relative corrections. In Sec. IV we give our conclusion.

*bondarenko@jinr.ru
†Also at Institute for Nuclear Problems, Belarusian State University, Minsk, 220006 Belarus.
‡Also at Institute of Physics, Southern Federal University, Rostov-on-Don, 344090 Russia.

II. DIFFERENTIAL CROSS SECTION

Let us consider scattering of longitudinally polarized e^+ and e^- beams with polarization degrees P_{e^+} and P_{e^-}, respectively. Then the cross section of the generic process $e^+e^- \to \ldots$ can be expressed as follows:

$$\sigma(P_{e^-}, P_{e^+}) = \frac{1}{4}\sum_{\chi_1,\chi_2}(1+\chi_1 P_{e^+})(1+\chi_2 P_{e^-})\sigma_{\chi_1\chi_2}, \quad (1)$$

where $\chi_i = -1(+1)$ corresponds to a lepton with left (right) helicity.

The complete one-loop cross section of the process can be divided into four parts:

$$\sigma^{\text{one-loop}} = \sigma^{\text{Born}} + \sigma^{\text{virt}}(\lambda) + \sigma^{\text{soft}}(\lambda,\omega) + \sigma^{\text{hard}}(\omega), \quad (2)$$

where σ^{Born} is the Born cross section, σ^{virt} is the contribution of virtual (loop) corrections, and $\sigma^{\text{soft(hard)}}$ is the soft (hard) photon emission contribution (where the hard photon energy $E_\gamma > \omega$). The auxiliary parameters λ ("photon mass") and ω are canceled after summation.

We apply the helicity approach to all contributions.

The virtual (Born) cross section of the $e^+e^- \to ZH$ process

$$e^+(p_1,\chi_1) + e^-(p_2,\chi_2) \to Z(p_3,\chi_3) + H(p_4) \quad (3)$$

can be written as follows:

$$\frac{d\sigma^{\text{virt(Born)}}_{\chi_1\chi_2}}{d\cos\vartheta_Z} = \frac{\sqrt{\lambda(s,M_Z^2,M_H^2)}}{32\pi s^2}|\mathcal{H}^{\text{virt(Born)}}_{\chi_1\chi_2}|^2, \quad (4)$$

where

$$|\mathcal{H}^{\text{virt(Born)}}_{\chi_1\chi_2}|^2 = \sum_{\chi_3=0,\pm1}|\mathcal{H}^{\text{virt(Born)}}_{\chi_1\chi_2\chi_3}|^2. \quad (5)$$

The soft bremsstrahlung term is factorized in front of the Born cross section as follows:

$$\frac{d\sigma^{\text{soft}}_{\chi_1\chi_2}}{d\cos\vartheta_Z} = \frac{d\sigma^{\text{Born}}_{\chi_1\chi_2}}{d\cos\vartheta_Z}\cdot\frac{\alpha}{2\pi}\left(-L_s^2 + 4L_s\ln\frac{2\omega}{\lambda} - \frac{2\pi^2}{3} + 1\right),$$
$$L_s = \ln\frac{s}{m_e^2} - 1. \quad (6)$$

The cross section for the hard bremsstrahlung

$$e^+(p_1,\chi_1) + e^-(p_2,\chi_2) \to Z(p_3,\chi_3) + H(p_4) + \gamma(p_5,\chi_5) \quad (7)$$

is given by the expression

$$\frac{d\sigma^{\text{hard}}_{\chi_1\chi_2}}{ds'd\cos\theta_4 d\phi_4 d\cos\theta_5} = \frac{s-s'}{8(4\pi)^4 ss'}\frac{\sqrt{\lambda(s',M_Z^2,M_H^2)}}{\sqrt{\lambda(s,m_e^2,m_e^2)}}|\mathcal{H}^{\text{hard}}_{\chi_1\chi_2}|^2, \quad (8)$$

where $s' = (p_3+p_4)^2$ and

$$|\mathcal{H}^{\text{hard}}_{\chi_1\chi_2}|^2 = \sum_{\chi_3=0,\pm1}\sum_{\chi_5=\pm1}|\mathcal{H}^{\text{hard}}_{\chi_1\chi_2\chi_3\chi_5}|^2. \quad (9)$$

Here θ_5 is the angle between the 3-momenta of the photon and positron, θ_4 is the angle between the 3-momenta of the Z boson and photon in the rest frame of the (Z,H) compound, and ϕ_4 is the azimuthal angle of the Z boson in the rest frame of the (Z,H) compound.

A. Covariant amplitude for the Born and virtual parts

Neglecting the masses, the CA of the initial particles can be written as follows [27]:

$$\mathcal{A}^{eeZH} = N(s)\Bigg\{\Bigg[\bar{v}(p_1)\Bigg(\gamma_\nu\gamma_+\sigma_e\mathcal{F}_0^+(s,t)$$
$$+\sum_{i=1,2}\not{p}_3\gamma_+(p_i)_\nu\mathcal{F}_i^+(s,t)\Bigg)u(p_2)\varepsilon_\nu^Z(p_3)\Bigg]$$
$$+[\sigma_e\to\delta_e, \gamma_+\to\gamma_-, \mathcal{F}_i^+(s,t)\to\mathcal{F}_i^-(s,t)]\Bigg\}, \quad (10)$$

where

$$N(s) = \frac{ig^2}{4c_W^2}\frac{M_Z}{s - M_Z^2 + iM_Z\Gamma_Z}. \quad (11)$$

We have also used various coupling constants:

$$\sigma_e = v_e + a_e, \qquad \delta_e = v_e - a_e,$$
$$c_W = \frac{M_W}{M_Z}, \qquad g = \frac{e}{s_W}. \quad (12)$$

B. Helicity amplitudes for the Born and virtual parts

There are six nonzero HAs for the virtual contribution:

$$\mathcal{H}_{+-+} = N(s)\sqrt{\frac{s}{2}}c_+\Big\{\sqrt{\lambda}c_-[\mathcal{F}_2^+(s,t)$$
$$-\mathcal{F}_1^+(s,t)] - 4\sigma_e\mathcal{F}_0^+(s,t)\Big\},$$
$$\mathcal{H}_{+--} = N(s)\sqrt{\frac{s}{2}}c_-\Big\{\sqrt{\lambda}c_+[\mathcal{F}_2^+(s,t)$$
$$-\mathcal{F}_1^+(s,t)] - 4\sigma_e\mathcal{F}_0^+(s,t)\Big\},$$
$$\mathcal{H}_{+-0} = N(s)L\frac{\sin\vartheta_z}{2M_Z}\Big\{\sqrt{\lambda}[\beta_+\mathcal{F}_1^+(s,t)$$
$$+\beta_-\mathcal{F}_2^+(s,t)] + 4\sigma_e\mathcal{F}_0^+(s,t)\Big\}, \quad (13)$$

where

$$L = s + M_Z^2 - M_H^2, \qquad \lambda = \lambda(s, M_Z^2, M_H^2),$$
$$\beta = \beta(s, M_Z^2, M_H^2) = \frac{\sqrt{\lambda}}{L}, \qquad \beta_\pm = \beta \pm \cos\vartheta_Z,$$
$$c_\pm = 1 \pm \cos\vartheta_Z. \tag{14}$$

The expression for the amplitude $\mathcal{H}_{-++}$ ($\mathcal{H}_{-+-}$) can be obtained from the expression for $\mathcal{H}_{+-+}$ ($\mathcal{H}_{+--}$) by replacing $\sigma_e \to \delta_e, c_+ \to c_-, \mathcal{F}^+ \to \mathcal{F}^-$, and the amplitude $\mathcal{H}_{-+0}$ can be obtained from $-\mathcal{H}_{+-0}$ by replacing $\sigma_e \to \delta_e$.

The form factors should be set to $\mathcal{F}_0^\pm(s,t) = 1$ and $\mathcal{F}_i^\pm(s,t) = 0$ in order to get Born HAs.

C. Helicity amplitudes for hard bremsstrahlung

We introduce the following notations for the massless particle spinors with light-like momentum k_i:

$$\begin{aligned}
u_+(k_i) &= \gamma_+ u(k_i) = v_-(k_i) = \gamma_+ v(k_i) = |i\rangle,\\
u_-(k_i) &= \gamma_- u(k_i) = v_+(k_i) = \gamma_- v(k_i) = |i],\\
\bar{u}_+(k_i) &= \bar{u}(k_i)\gamma_- = \bar{v}_-(k_i) = \bar{v}(k_i)\gamma_- = [i|,\\
\bar{u}_-(k_i) &= \bar{u}(k_i)\gamma_+ = \bar{v}_+(k_i) = \bar{v}(k_i)\gamma_+ = \langle i|.
\end{aligned} \tag{15}$$

Using Eq. (15) we construct the polarization wave functions for other particles, including the massive ones.

We project all massive momenta with $p_i^2 = m_i^2$ to the light cone of the photon p_5 and introduce the associated "momenta":

$$\begin{aligned}
k_i &= p_i - \frac{m_i^2}{2p_i \cdot p_5} p_5, \qquad k_i^2 = 0, \qquad i = 1\ldots4,\\
k_5 &= -\sum_{i=1}^4 k_i = K p_5,\\
K &= 1 + \sum_{i=1}^4 \frac{m_i^2}{2p_i \cdot p_5} = 1 + \sum_{i=1}^4 \frac{m_i^2}{2k_i \cdot p_5},\\
p_5 &= -\sum_{i=1}^4 p_i = K' k_5,\\
K' &= 1 - \sum_{i=1}^4 \frac{m_i^2}{2p_i \cdot k_5} = 1 - \sum_{i=1}^4 \frac{m_i^2}{2k_i \cdot k_5}.
\end{aligned} \tag{16}$$

Since the vector k_5 appears to be light-like, there is a certain "momentum conservation" of the associated vectors.

To construct the photon polarization vector and fix the gauge parameters, we need to introduce the auxiliary massless vector q. We use the following parametrization:

$$\begin{aligned}
\varepsilon_\mu^+(k_5) &= \frac{\langle q|\gamma_\mu|5]}{\sqrt{2}\langle q5\rangle},\\
\varepsilon_\mu^-(k_5) &= \frac{[q|\gamma_\mu|5\rangle}{\sqrt{2}[q5]} = (\varepsilon_\mu^+(k_5))^*,\\
\hat{\varepsilon}^+(k_5) &= \gamma^\mu \varepsilon_\mu^+(k_5) = \sqrt{2}\frac{|q\rangle[5| + |5]\langle q|}{\langle q5\rangle},\\
\hat{\varepsilon}^-(k_5) &= \sqrt{2}\frac{|q]\langle 5| + |5\rangle[q|}{[q5]}.
\end{aligned} \tag{17}$$

There are 20 nonzero HAs for hard bremsstrahlung:

$$\begin{aligned}
A^{\text{hard}}_{--++} &= 2m_e M_Z \frac{[12]\langle 35\rangle}{[35]}\left(\frac{\delta_e}{s_{15}} + \frac{\sigma_e}{s_{25}}\right),\\
A^{\text{hard}}_{++-+} &= 2m_e M_Z \frac{[12][35]\langle 15\rangle\langle 25\rangle}{\langle 35\rangle[15][25]}\left(\frac{\sigma_e}{s_{15}} + \frac{\delta_e}{s_{25}}\right),\\
A^{\text{hard}}_{-+-+} &= -2M_Z \frac{\sigma_e}{s_{15}} \frac{[12][13]\langle 15\rangle\langle 25\rangle}{\langle 35\rangle[25]},\\
A^{\text{hard}}_{+--+} &= -2M_Z \frac{\delta_e}{s_{25}} \frac{[12][23]\langle 25\rangle\langle 15\rangle}{\langle 35\rangle[15]},\\
A^{\text{hard}}_{--0+} &= \sqrt{2}m_e [12]\langle 35\rangle\left(\frac{\delta_e}{s_{15}}\frac{[23]}{[25]} + \frac{\sigma_e}{s_{25}}\frac{[13]}{[15]}\right),\\
A^{\text{hard}}_{-+++} &= -2M_Z\sigma_e\left(\frac{[12]\langle 23\rangle\langle 25\rangle}{s_{25}[35]} + \frac{[15]\langle 35\rangle}{[25][35]}\right),\\
A^{\text{hard}}_{+-++} &= -2M_Z\delta_e\left(\frac{[12]\langle 13\rangle\langle 15\rangle}{s_{15}[35]} - \frac{[25]\langle 35\rangle}{[15][35]}\right),\\
A^{\text{hard}}_{++0+} &= \sqrt{2}m_e\frac{[35]}{[15][25]}\Bigg(\langle 35\rangle 2a_e\\
&\quad + [12]\left(\frac{\sigma_e}{s_{15}}\langle 15\rangle\langle 23\rangle + \frac{\delta_e}{s_{25}}\langle 25\rangle\langle 13\rangle\right)\Bigg),\\
A^{\text{hard}}_{-+0+} &= -\sqrt{2}\frac{[12]}{[25]}\Bigg(\delta_e\frac{m_e^2 s_{45}\langle 25\rangle}{s_{15}s_{25}}\\
&\quad + \sigma_e\left(\frac{[13]\langle 23\rangle\langle 15\rangle}{s_{15}} + \frac{[13]\langle 35\rangle}{[12]} + \frac{M_Z^2\langle 25\rangle}{s_{45}}\right)\Bigg),\\
A^{\text{hard}}_{+-0+} &= -\sqrt{2}\frac{[12]}{[15]}\Bigg(\sigma_e\frac{m_e^2 s_{45}\langle 15\rangle}{s_{15}s_{25}}\\
&\quad + \delta_e\left(\frac{[23]\langle 13\rangle\langle 25\rangle}{s_{25}} - \frac{[23]\langle 35\rangle}{[12]} + \frac{M_Z^2\langle 15\rangle}{s_{45}}\right)\Bigg),
\end{aligned}$$

where

$$s_{i5} = 2k_i \cdot p_5 = K'\langle i5\rangle[5i].$$

The other HAs ones can be obtained by using *CP* symmetry:

$$A^{\text{hard}}_{\chi_1\chi_2\chi_3\chi_5} = -\chi_1\chi_2\chi_3\chi_5 \bar{A}^{\text{hard}}_{-\chi_1-\chi_2-\chi_3-\chi_5}|_{p_1\leftrightarrow p_2}. \tag{18}$$

There is some degree of freedom in the choice of the light-cone projection which corresponds to the arbitrariness of the spin quantization direction. We use it to make the above expressions compact.

To obtain the amplitudes $\mathcal{H}$ with definite helicity, spin-rotation matrices C should be independently applied for each index χ of incoming particles:

$$\mathcal{H}_{\ldots\xi_i\ldots} = eN(s')C^{\chi_i}_{\xi_i}A_{\ldots\chi_i\ldots},$$

$$C^{\chi_i}_{\xi_i} = \begin{bmatrix} \frac{[k_{i^\flat}p_5]}{[p_ip_5]} & \frac{m_i\langle k_{i^*}p_5\rangle}{\langle k_{i^*}k_{i^\flat}\rangle\langle p_ip_5\rangle} \\ \frac{m_i[k_{i^*}p_5]}{[k_{i^*}k_{i^\flat}][p_ip_5]} & \frac{\langle k_{i^\flat}p_5\rangle}{\langle p_ip_5\rangle} \end{bmatrix} = \begin{bmatrix} \frac{\langle k_{i^*}p_i\rangle}{\langle k_{i^*}k_{i^\flat}\rangle} & \frac{m_i\langle k_{i^*}p_5\rangle}{\langle k_{i^*}k_{i^\flat}\rangle\langle p_ip_5\rangle} \\ \frac{m_i[k_{i^*}p_5]}{[k_{i^*}k_{i^\flat}][p_ip_5]} & \frac{[k_{i^*}p_i]}{[k_{i^*}k_{i^\flat}]} \end{bmatrix}, \tag{19}$$

where

$$k_{i^*} = \{|\vec{p}_i|, -p_i^x, -p_i^y, -p_i^z\}, \qquad k_{i^*}^2 = 0,$$
$$k_{i^\flat} = p_i - \frac{m_i^2}{2p_i\cdot k_{i^*}}k_{i^*}, \qquad k_{i^\flat}^2 = 0. \tag{20}$$

III. NUMERICAL RESULTS AND COMPARISON

In this section we present numerical results for polarized EW RCs to the $e^+e^- \to ZH$ process obtained by means of the MCSANCEE integrator. We work in the $\alpha(0)$ EW scheme and use the following set of input parameters:

$$\alpha^{-1}(0) = 137.03599976, \qquad \Gamma_Z = 2.49977\ \text{GeV}$$
$$M_W = 80.4514958\ \text{GeV}, \qquad M_Z = 91.1876\ \text{GeV},$$
$$M_H = 125\ \text{GeV}, \qquad m_e = 0.51099907\ \text{MeV},$$
$$m_\mu = 0.105658389\ \text{GeV}, \qquad m_\tau = 1.77705\ \text{GeV},$$
$$m_d = 0.083\ \text{GeV}, \qquad m_s = 0.215\ \text{GeV},$$
$$m_b = 4.7\ \text{GeV}, \qquad m_u = 0.062\ \text{GeV},$$
$$m_c = 1.5\ \text{GeV}, \qquad m_t = 173.8\ \text{GeV}. \tag{21}$$

In Ref. [27] we compared the one-loop EW calculations (excluding hard bremsstrahlung) with the results of Refs. [19,20] and the GRACE-LOOP program [24]. Good agreement has also been obtained between the Born and pure weak contributions and the results of Refs. [16,17].

The polarized Born and hard bremsstrahlung cross sections are verified by means of the corresponding results of the WHIZARD [25] and CALCHEP [26] programs. For comparison of the real photon emission we apply an additional cut on the photon energy $E_\gamma > 1$ GeV. We obtain an excellent agreement with the above-mentioned programs.

To calculate the one-loop EW RCs we use the soft-hard separator $\omega \ll \sqrt{s}/2$.

TABLE I. Hard ($E_\gamma > 1$ GeV), Born, and one-loop cross sections in fb and relative corrections δ in % for the c.m. energy $\sqrt{s} = 250$ GeV and various polarization degrees of the initial particles.

P_{e^-}	P_{e^+}	σ^{hard}, fb	σ^{Born}, fb	$\sigma^{\text{one-loop}}$, fb	δ, %
0	0	82.0(1)	225.59(1)	206.77(1)	−8.3(1)
−0.8	0	96.7(1)	266.05(1)	223.33(2)	−16.1(1)
−0.8	−0.6	46.3(1)	127.42(1)	111.67(2)	−12.4(1)
−0.8	0.6	147.1(1)	404.69(1)	334.99(1)	−17.2(1)

TABLE II. Hard ($E_\gamma > 1$ GeV), Born, and one-loop cross sections in fb and relative corrections δ in % for the c.m. energy $\sqrt{s} = 500$ GeV and various polarization degrees of the initial particles.

P_{e^-}	P_{e^+}	σ^{hard}, fb	σ^{Born}, fb	$\sigma^{\text{one-loop}}$, fb	δ, %
0	0	38.95(1)	53.74(1)	62.42(1)	16.7(1)
−0.8	0	45.92(1)	63.38(1)	68.31(1)	7.8(1)
−0.8	−0.6	22.10(1)	30.35(1)	34.04(1)	12.1(1)
−0.8	0.6	69.74(1)	96.40(1)	102.58(1)	6.4(1)

Tables I–III show the results for the polarized Born, hard bremsstrahlung, and one-loop cross sections (in fb), and the relative corrections for various c.m. energies and polarization degrees of the initial particles. The relative correction δ (in %) is defined as follows:

$$\delta = \frac{\sigma^{\text{one-loop}}(P_{e^-}, P_{e^+})}{\sigma^{\text{Born}}(P_{e^-}, P_{e^+})} - 1. \tag{22}$$

In Table I we present the hard ($E_\gamma > 1$ GeV), Born, and one-loop cross sections in fb and relative corrections δ in % for a c.m. energy $\sqrt{s} = 250$ GeV and various polarization degrees of the initial particles. For the unpolarized case the correction is negative and equal to about −8%. It remains negative and reaches its highest value of about −17% for the polarization values $(P_{e^-}, P_{e^+}) = (-0.8, 0.6)$.

In Tables II and III we present cross sections and relative corrections for the c.m. energies $\sqrt{s} = 500$, 1000 GeV. The unpolarized corrections are positive and equal to about 17% for $\sqrt{s} = 500$ GeV and 21% for $\sqrt{s} = 1000$ GeV. The polarized corrections remain positive and reach their lowest

TABLE III. Hard ($E_\gamma > 1$ GeV), Born, and one-loop cross sections in fb and relative corrections δ in % for the c.m. energy $\sqrt{s} = 1000$ GeV and various polarization degrees of the initial particles.

P_{e^-}	P_{e^+}	σ^{hard}, fb	σ^{Born}, fb	$\sigma^{\text{one-loop}}$, fb	δ, %
0	0	11.67(1)	12.05(1)	14.56(1)	20.8(1)
−0.8	0	13.75(1)	14.217(1)	15.80(1)	11.1(1)
−0.8	−0.6	6.65(1)	6.809(1)	7.95(1)	16.7(1)
−0.8	0.6	20.85(1)	21.62(1)	23.66(1)	9.4(1)

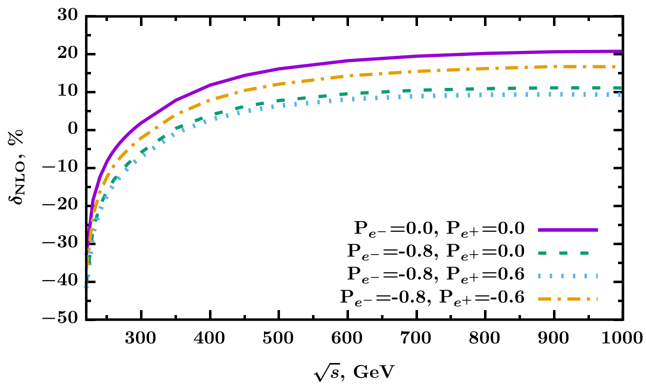

FIG. 1. The complete one-loop relative corrections δ for various polarization degrees.

values of about 6% for $\sqrt{s} = 500$ GeV and 9% for $\sqrt{s} = 1000$ GeV for the polarization values $(P_{e^-}, P_{e^+}) = (-0.8, 0.6)$.

Figure 1 shows the complete one-loop relative corrections of various polarization degrees of the initial particles. The notations are as follows: $(P_{e^-}, P_{e^+}) = (0, 0)$ (solid violet line), $(-0.8, 0)$ (dashed green line), $(-0.8, 0.6)$ (dotted blue line), and $(-0.8, -0.6)$ (dash-dotted orange line).

The comparison of cross sections between the unpolarized and polarized cases demonstrates the significance of the polarization effects.

In Fig. 2 the separate pure weak (PW), QED, and one-loop (NLO) contributions to the relative corrections are shown, where

$$\delta_{\rm NLO} = \delta_{\rm PW} + \delta_{\rm QED}. \tag{23}$$

The lines corresponding to different contributions and schemes are labeled as follows: NLO $\alpha(0)$ (solid violet line), PW $\alpha(0)$ (dotted green line), NLO G_μ (dashed green line), PW G_μ (dash-dotted orange line), and QED (dash-dot-dotted blue line). The QED contribution has the largest impact on the relative correction in comparison with the pure weak term. The G_μ EW scheme calculations are shifted by $-(6–7)\%$ in comparison with the $\alpha(0)$ scheme.

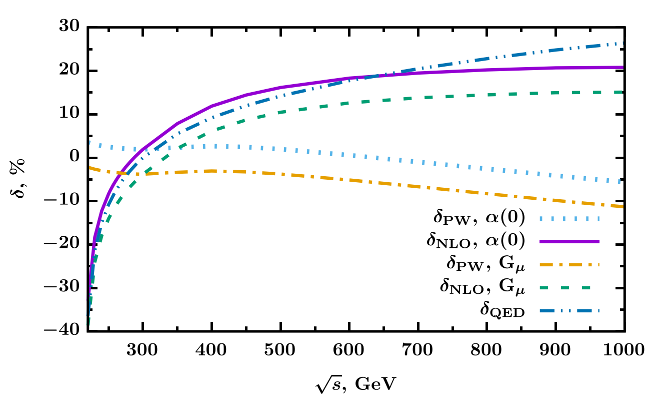

FIG. 2. Relative corrections δ in percent of NLO, PW, and QED contributions in the $\alpha(0)$ and G_μ EW schemes.

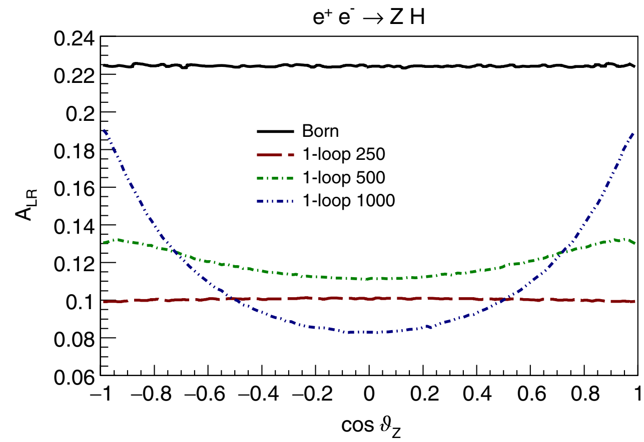

FIG. 3. Distributions of the left-right asymmetry A_{LR} in $\cos\vartheta_Z$ for the Born and one-loop levels for the c.m. energies $\sqrt{s} = 250$, 500, 1000 GeV.

Figure 3 shows the distributions of the left-right asymmetry A_{LR} in $\cos\vartheta_Z$ for the Born and one-loop levels for the c.m. energies $\sqrt{s} = 250$, 500, 1000 GeV, where A_{LR} is defined as follows:

$$A_{LR} = \frac{\sigma(-1,1) - \sigma(1,-1)}{\sigma(-1,1) + \sigma(1,-1)}. \tag{24}$$

At the Born level the A_{LR} is constant:

$$A_{LR}^{\rm Born} = \frac{-3M_Z^4 + 4M_Z^2 M_W^2}{5M_Z^4 - 12M_Z^2 M_W^2 + 8M_W^4} = 0.2243. \tag{25}$$

The asymmetry analysis (Fig. 3) shows a significant increase of A_{LR} at high angles as the c.m. energy increases from $\sqrt{s}$ from 250 GeV to 1000 GeV.

The next-to-next-to-leading-order mixed QCD-EW $\mathcal{O}(\alpha\alpha_s)$ corrections to the unpolarized integrated cross sections were estimated in Refs. [16,17]. They are about 1% in the region of c.m. energy $\sqrt{s} = 250$–500 GeV in the $\alpha(0)$ EW scheme and, at least, 1 order of magnitude lower in comparison with the complete $\mathcal{O}(\alpha)$ corrections.

IV. CONCLUSION AND OUTLOOK

In the paper we have investigated the complete one-loop electroweak radiative corrections for the process $e^+e^- \to ZH$ with longitudinal polarization of positron and electron beams in a wide center-of-mass energy range.

We have reported estimations for the relative corrections δ for various values of the longitudinal polarization of the positron and electron beams for various energy values: for 250, 500, and 1000 GeV the relative corrections are -8.3 to -17.2%, 6.4 to 16.7%, and 9.4 to 20.8%, respectively.

Note that a sharp increase of the relative correction δ (see Fig. 1) at the threshold is due to the small absolute values of the Born and one-loop contributions. The δ is of the order of 20% at 1 TeV and represents the combination of the large positive QED and small negative weak corrections. The QED corrections dominate in this energy region.

When calculating the asymmetry, the factorizable corrections (such as QED) are mutually reduced. Thus, we see that the magnitude of the asymmetry is sensitive to the contributions from nonfactorizable corrections, such as those from the weak sector. Therefore, understanding the asymmetry may be helpful in searching for new physics [28–30].

All numerical calculations have been performed using the MCSANCEE integrator which allows one to calculate differential, integrated cross sections and distributions for $e^+e^- \to e^+e^-, ZH$ reactions with the longitudinally polarized positron and electron beams. In addition the integrator, the MCSANCEE event generator at the complete one-loop level currently being developed [31].

It is important to emphasize that for experimental investigations the higher-order corrections (mixed QCD-EW corrections, Sudakov two-loop leading logarithms, multiphoton resummation, and so on) should also be included in the precise theoretical tools.

ACKNOWLEDGMENTS

The results have been obtained within the framework of the state task N 3.9696.2017/8.9 from the Ministry of Education and Science of Russia.

[1] G. Moortgat-Pick *et al.*, Phys. Rep. **460**, 131 (2008).
[2] ILC Technical Design Report Vol. **1**, edited by T. Behnke, J. E. Brau, B. Foster, J. Fuster, M. Harrison, J. McEwan Paterson, M. Peskin, M. Stanitzki, N. Walker, and H. Yamamoto, https://arxiv.org/abs/1306.6327.
[3] A Multi-TeV Linear Collider Based on CLIC Technology: CLIC Conceptual Design Report, edited by M. Aicheler, P. Burrows, M. Draper, T. Garvey, P. Lebrun, K. Peach, N. Phinney, H. Schmickler, D. Schulte, and N. Toge, Reports No. CERN-2012-007, No. SLAC-R-985, No. KEK-Report-2012-1, No. PSI-12-01, and No. JAI-2012-001.
[4] CEPC Study Group, CEPC Conceptual Design Report Vol. **1**—Accelerator, https://arxiv.org/abs/1809.00285.
[5] A. Abada *et al.*, Eur. Phys. J. Spec. Top. **228**, 261 (2019).
[6] A. Arbuzov, S. Bondarenko, Ya. Dydyshka, L. Kalinovskaya, and R. Sadykov, The SANC project, in *Mini Workshop on Precision EW and QCD Calculations for the FCC Studies: Methods and Techniques CERN*, 2018 (CERN, Geneva, 2018), https://arxiv.org/pdf/1809.01830.pdf#section.3.7.
[7] A. Blondel and P. Janot, arXiv:1809.10041.
[8] A. Arbuzov, S. Bondarenko, Y. Dydyshka, L. Kalinovskaya, L. Rumyantsev, R. Sadykov, and V. Yermolchyk, Electron-positron annihilation processes in MCSANCee, in *Theory Report on the 11th FCC-ee Workshop* (CERN, Geneva, 2019), https://arxiv.org/pdf/1905.05078.pdf.
[9] G. J. Gounaris and F. M. Renard, Phys. Rev. D **90**, 073007 (2014).
[10] R. Lafaye, T. Plehn, M. Rauch, and D. Zerwas, Phys. Rev. D **96**, 075044 (2017).
[11] V. D. Barger, K.-m. Cheung, A. Djouadi, B. A. Kniehl, and P. M. Zerwas, Phys. Rev. D **49**, 79 (1994).
[12] E. Accomando *et al.* (ECFA/DESY LC Physics Working Group), Phys. Rep. **299**, 1 (1998).
[13] J. Fleischer and F. Jegerlehner, Nucl. Phys. **B216**, 469 (1983).
[14] J. Fleischer and F. Jegerlehner, Nucl. Phys. **B228**, 1 (1983).
[15] B. A. Kniehl, Z. Phys. C **55**, 605 (1992).
[16] Y. Gong, Z. Li, X. Xu, L. L. Yang, and X. Zhao, Phys. Rev. D **95**, 093003 (2017).
[17] Q.-F. Sun, F. Feng, Y. Jia, and W.-L. Sang, Phys. Rev. D **96**, 051301 (2017).
[18] M. Greco, G. Montagna, O. Nicrosini, F. Piccinini, and G. Volpi, Phys. Lett. B **777**, 294 (2018).
[19] A. Denner, Nucl. Phys. B, Proc. Suppl. **29A**, 263 (1992).
[20] A. Denner, J. Kublbeck, R. Mertig, and M. Bohm, Z. Phys. C **56**, 261 (1992).
[21] D. Bardin, S. Bondarenko, P. Christova, L. Kalinovskaya, L. Rumyantsev, A. Sapronov, and W. von Schlippe, JETP Lett. **96**, 285 (2012).
[22] A. Arbuzov, D. Bardin, S. Bondarenko, P. Christova, L. Kalinovskaya, U. Klein, V. Kolesnikov, L. Rumyantsev, R. Sadykov, and A. Sapronov, JETP Lett. **103**, 131 (2016).
[23] D. Bardin, Y. Dydyshka, L. Kalinovskaya, L. Rumyantsev, A. Arbuzov, R. Sadykov, and S. Bondarenko, Phys. Rev. D **98**, 013001 (2018).
[24] G. Belanger, F. Boudjema, J. Fujimoto, T. Ishikawa, T. Kaneko, K. Kato, and Y. Shimizu, Phys. Rep. **430**, 117 (2006).
[25] W. Kilian, S. Brass, T. Ohl, J. Reuter, V. Rothe, P. Stienemeier, and M. Utsch, New developments in WHIZARD version 2.6, in *International Workshop on Future Linear Collider (LCWS2017) Strasbourg, France, 2017* (2018).
[26] A. Belyaev, N. D. Christensen, and A. Pukhov, Comput. Phys. Commun. **184**, 1729 (2013).
[27] D. Bardin, S. Bondarenko, L. Kalinovskaya, G. Nanava, L. Rumyantsev, and W. von Schlippe, Comput. Phys. Commun. **177**, 738 (2007).
[28] K. Fujii *et al.*, arXiv:1506.05992.
[29] K. Fujii *et al.*, arXiv:1710.07621.
[30] P. Bambade *et al.*, arXiv:1903.01629.
[31] MCSANCee event generator, CPC (to be published).